

PHYSICO-CHEMICAL PROPERTIES OF MICROARC OXIDATION OF BIOCOMPATIBLE COATINGS ON TITANIUM: INFLUENCE OF ELECTROCHEMISTRY PARAMETERS

Maria Magdalena DICU¹, Marioara ABRUDEANU², Jean-Pierre MILLET³
Sorin MOGA⁴, Vasile RIZEA⁵, Cătălin DUCU⁶

Cele mai importante proprietăți fizico-chimice ale materialelor cu aplicații biomedicale sunt: morfologia, structura cristalină și rezistența la coroziune. În această lucrare urmărim evoluția acestor proprietăți, în funcție de condițiile de obținere a straturilor de TiO₂. Aceste straturi au fost realizate prin tehnica oxidării în microarc (MAO) pe suport de titan. Electrolitul folosit este un amestec format din β-gliceroftosfat disodic pentahidratat și acetat de calciu. Straturile obținute sunt caracterizate prin microscopie electronică de baleaj, difracție cu radiații X și teste de coroziune. Proprietățile anticorozive ale straturilor au fost testate prin impedanță electrochimică, voltametrie ciclică și teste Tafel, în soluție tampon. Rezultatele demonstrează o bună stabilitate electrochimică, combinată cu rezultate pozitive cu privire la biocompatibilitate.

The most important physico-chemical properties of materials with biomedical applications are: the morphology, the surface structure and the corrosion resistance. In this paper we follow the evolution of these properties, according to the conditions for obtaining TiO₂ coatings. These coatings were formed on titanium substrate by microarc oxidation (MAO). The electrolyte is a mixture consisting of β-glycerophosphate disodium salt pentahydrate and calcium acetate monohydrate. The obtained surfaces were characterized using scanning electron microscopy, X-rays analysis and corrosion tests. The anticorrosion properties of the layers were tested in biological environment (buffer solution) by means of electrochemical impedance spectroscopy (EIS), cyclic voltammetry, Tafel tests. The results show a good electrochemical stability, combined with positive results regarding their biocompatibility.

¹ Project manager, Research Centre For Advanced Materials – University of Pitesti, e-mail: ela_magda@yahoo.com

² Prof., Department of Technology and Management, University of Pitesti, e-mail: abrudeanu@upit.ro

³ Prof., MATEIS, INSA, Lyon, France, e-mail: jean-pierre.millet@insa-lyon.fr

⁴ PhD Student, Research Centre For Advanced Materials – University of Pitesti, e-mail: sorin.moga@upit.ro

⁵ Lect., Department of Technology and Management, University of Pitesti, e-mail: rizeav@hotmail.com

⁶ CS III, Research Centre For Advanced Materials – University of Pitesti, e-mail: catalin.ducu@upit.ro

Keywords: titania, microarc oxidation, surface analysis, electrochemical stability

1. Introduction

Titanium and titanium alloys are adequate materials for dental and orthopedic implants or prostheses due to their corrosion resistance, biocompatibility, durability and strength. A major impediment of such implants is their bioinertness [1–4]. Therefore, a range of physical and chemical treatments of the titanium surface have been proposed to obtain improved osteointegration.

Microarc oxidation (MAO), also known as plasma electrolytic oxidation or anodic spark oxidation is a relatively convenient technique to improve the bioactivity of titanium implants by forming bioactive coatings [5–8]. MAO is considered one of the most useful method for surface modification, because it can produce porous and firmly adherent TiO_2 films on titanium implants [9,10].

The key role of titanium oxide layer is to enhance the bone-bonding ability of Ti implants, i.e. osteoconductivity [11]. The oxide layer formed by anodic reaction has a barrier type structure inside and a porous structure outside [12,13].

An advantage of MAO is that the composition of the coatings can be designed by using electrolytes with specific compositions. Elements such as Ca and P have been confirmed to promote the bioactivity of implants [14–19]. Well-adhered coatings on metal surfaces with complex geometry such as screw-shape titanium implants can be obtained with MAO [16].

The growth of coatings under MAO conditions enables modification of oxide properties compared with conventional anodizing below the sparking voltage, such as thickness, crystal structure, chemical composition, topography, porosity, and roughness, [20] which have been shown to influence the bone response [21,22]. Sul *et al.* demonstrated that strong reinforcement of bone tissue reactions occurs with anatase-containing coatings >600 nm thick, with a porous surface morphology [21]. The structures of anodic films and MAO coatings on titanium are greatly affected by species incorporated into the coating from the electrolyte, with crystallinity being suppressed in silicon-containing coatings, phosphorus and calcium species [23–28].

In this paper, experimental results on the elaboration of TiO_2 coatings on commercially titanium by MAO are categorized and explained. The morphology, phase component and corrosion resistance of the oxide layers were characterized by SEM, XRD, electrochemical impedance spectroscopy, Tafel plots, and cyclic voltammetry.

2. Experimental Details

2.1. Materials and Methods

Titanium specimens were cut from a sheet of titanium (commercially pure titanium - grade 2) and used as substrate. The chemical composition of the raw material is: Fe 0.105 %; C 0.011 %; O 0.175 %; N 0.006 %; H 0.0005 % and balance Ti. The titanium plates were polished using #200 – #1000 SiC sandpaper gradually, degreased and successively cleaned in an ultrasonic bath with ethyl alcohol and distilled water. The Ti plates were anodized in an electrolytic solution containing 0.04 mol/l β -glycerophosphate disodium salt pentahydrate ($C_3H_7Na_2O_6P \cdot 5H_2O$) and 0.3 mol/l calcium acetate monohydrate ($(CH_3COO)_2Ca \cdot H_2O$), by applying a pulsed DC field to the specimens.

The MAO equipment was designed and manufactured at the University of Pitesti within the Research Center for Advanced Materials. The experimental set-up consists of: an insulated stainless steel electrolyte cell with a stirrer and a pulsed DC power supply. The titanium plate was used as anode, while the stainless steel cell was used as cathode.

MAO was carried out at an applied voltage of 350 V for 3, 5, 7 and 10 min. The MAO treatments were carried out using a pulsed current regime. During the oxidation, the temperature of the electrolyte was less than 50°C. After the treatment, the samples were washed with distilled water and dried at room temperature.

2.2. Evaluation Techniques

The microstructures on the sample surfaces were observed by scanning electron microscopy (SEM; Low-vaccum Inspect S – FEI Company).

The surface structure of the films was analyzed by X-ray diffraction (XRD; Rigaku Ultima IV) using $CuK\alpha$ radiation, with Parallel Beam optics, in grazing incidence geometry (angle of incidence was kept constant at 1°). The measurements were conducted in the 2θ range 20^0 - 73^0 , step width 0.05^0 and 2s as counting time.

The corrosion resistance was determined by electrochemical methods in a buffer solution, at room temperature. The chemical composition of the solution was: NaCl 8.74 g/L; NaHCO₃ 0.35 g/L; Na₂HPO₄•12H₂O 0.06 g/L; NaH₂PO₄ 0.06 g/L.

The following techniques were employed:

- Tafel Plots. Polarization curves were recorded between ± 150 mV and free potential, at a scan rate of 2 mV/s. Prior to measurements, the specimens were

maintained in the solution for 30min. The following main electrochemical parameters were calculated from Tafel plots: i_{cor} = corrosion current density; R_p =polarization resistance; E_{cor} = corrosion potential; V_{cor} = corrosion rate.

- Electrochemical Impedance Spectroscopy (EIS). The EIS measurements were performed at free potential in buffer solution and in the 0.01-10.000 Hz frequency domain, with amplitude of ± 10 mV (rms). EIS analysis was discussed in term of Nyquist representation.

- Cyclic Voltammetry. Cyclic curves were recorded using buffer solution as an electrolyte. The electrode potential was cycled between -600 mV and $+4000$ mV, at a scan rate of 20 mV/s.

All electrochemical measurements were performed using one compartment cell with three electrodes: a working electrode, a platinum counter-electrode and an Ag/AgCl, KCl reference electrode connected to Autolab PGSTAT 302N potentiostat with NOVA general-purpose electrochemical system software.

3. Results and Discussion

3.1. Microstructures and Phase Composition of MAO Coatings

Fig. 1 shows SEM surface micrographs of the oxidized samples at 350 V for a) 3 and b) 5 minutes.

After MAO treatment, a porous titania film was formed on the titanium surface with numerous opened micropores. The pores diameters varied from 2 to 9 μ m. The holes in the surface were channels of micro-arc discharge in electrolyte. We can observe that the pore size increases with deposition time.

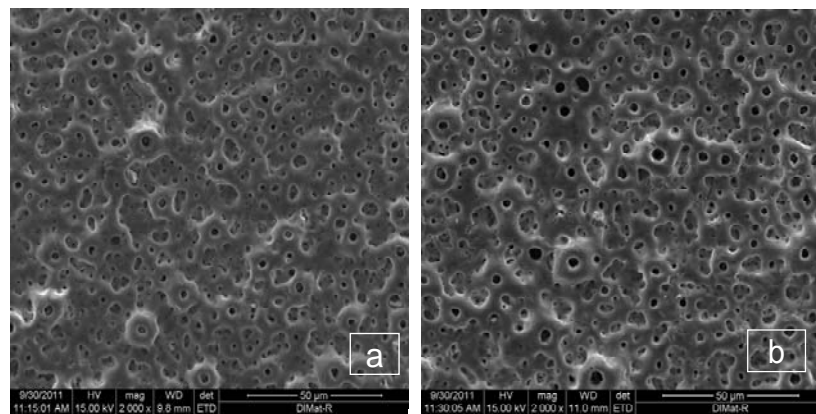


Fig. 1. SEM surface morphologies on titanium samples treated with MAO at 350 V for:
a. 3 min, b. 5 min

Usually, porous and rough surface morphology is a good feature for materials used in bio-applications. Pores in the film favors the anchorage of implants to bone and acts as nucleation sites for bone tissue.

Fig. 2 illustrates the GIXRD patterns of MAO treated samples for a) 3 min b) 5 min c) 10 min and d) 7 min. We can observe the presence of the titania phases (A- anatase and R-rutile) in the surface of the samples. As we expected, the intensity of anatase diffraction lines decreased with treatment time. Also, the alpha form of tricalcium phosphate phase was identified in all the analyzed samples.

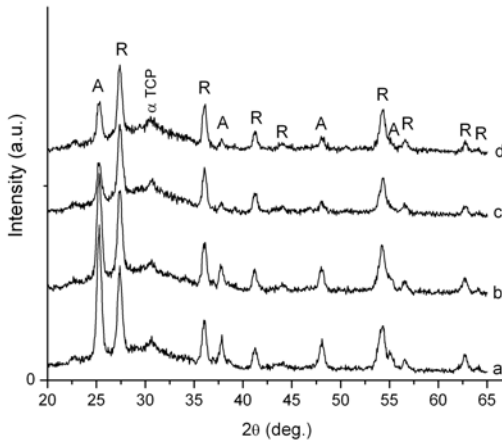


Fig. 2. GIXRD patterns of MAO samples a) 3 min b) 5 min c) 10 min d) 7 min

3.2. Electrochemical and Corrosion Characterization

3.2.1. Tafel Plots

The corrosion behavior of Ti/TiO₂ and titanium was estimated by Tafel plots in buffer solution and is illustrated in Fig. 3. To substantiate the anticorrosion properties, the Tafel regions of cathodic and anodic polarization curves are extrapolated.

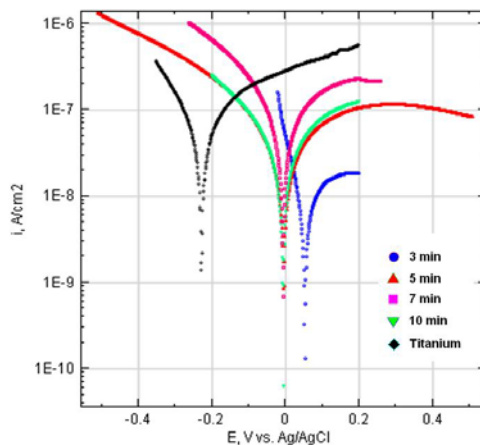


Fig. 3. Tafel plots recorded in buffer solution for titanium and Ti/TiO_2 surface layers

Table 1 shows the corrosion parameters and polarization resistances obtained from Tafel diagrams.

The corrosion rate of a sample is generally determined by the corrosion current and corrosion resistance [29, 30].

Table 1
Corrosion parameters and polarisation resistances obtained from Tafel diagrams

Sample	j_{cor} (A/cm^2)	R_p (Ω/cm^2)	E_{cor} (V)	V_{cor} (mm/year)
Titanium	$300,320 \times 10^{-9}$	$539,22 \times 10^3$	$-227,900 \times 10^{-3}$	0,00348
350 V / 3 min	$6,499 \times 10^{-9}$	$2,633 \times 10^6$	$56,942 \times 10^{-3}$	7,5528 E-5
350 V / 5 min	$248,320 \times 10^{-9}$	$1,25 \times 10^6$	$12,11 \times 10^{-3}$	0,0028
350 V / 7 min	$832,010 \times 10^{-9}$	$503,210 \times 10^3$	$-866,680 \times 10^{-6}$	0,00966
350 V / 10 min	$177,570 \times 10^{-9}$	$1,166 \times 10^6$	$-2,6226 \times 10^{-3}$	0,00206

The corrosion current density for titanium is 300 nA. After 3 minutes of MAO treatment the current density is 6 nA, which shows that surface was stabilized by a compact layer with a degree of porosity (as we observed in SEM micrographs). The pore size increases and the corrosion resistance decreases with the oxidation time. After 10 minutes the layer is more compact and the current density decreases under initial value of titanium sample.

Table 1 indicates that coated samples (excluding the sample treated for 7 min.) have a higher polarization resistance (R_p) due to a lower corrosion current density (j_{cor}) in comparison with that of the uncoated Ti.

3.2.2. Electrochemical Impedance Spectroscopy (EIS)

Electrochemical impedance spectroscopy (EIS) was also used to better analyze and compare the corrosion behavior of the coatings produced with different treatment time, as shown in Fig. 4. The EIS measurements are represented as Nyquist diagrams.

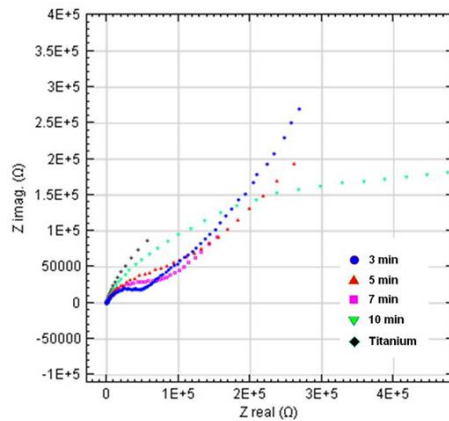


Fig. 4. Nyquist representation of experimental data for oxidized titanium with different treatment time and for titanium sample

The samples oxidized at 3, 5, 7 minutes by microarc oxidation show a diffuse behavior at low frequencies. After 10 minutes we can no longer observe this behavior, which means that the pores begin to close (the current density is more stable).

The EIS results indicated that the TiO_2 coatings have a bi-layered structure consisting of an inner barrier layer associated to high impedance and responsible for corrosion protection, and an outer porous layer, of lower impedance, which can facilitate the cell adhesion.

3.2.3. Cyclic Voltammetry

The electrochemical methods devoted to stability studies were completed with cyclic voltammetry curves obtained for our MAO coatings.

Fig. 5 shows the potential-current density curves, with a scan rate of 20 mV/s, for the four samples oxidized at 3, 5, 7, 10 min and 350V. The potentiodynamic curves obtained for MAO treatments are similar in shape. The return curves with negative values of density current, show the absence of local corrosion.

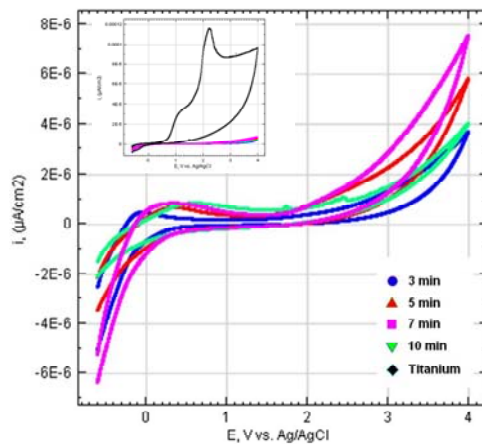


Fig. 5. Potentiodynamic curves obtained in buffer solution for titanium and for oxidized titanium by MAO at 350V

4. Conclusions

TiO_2 coatings grown on pure titanium surfaces by MAO method in electrolyte containing β -glycerophosphate disodium salt pentahydrate and calcium acetate monohydrate present a morphology and thickness that depend on the deposition time. The porous titania film present numerous opened micropores. The porous surface is beneficial to cell attachment and bone growth. Additionally, the presence of the porous coating could be beneficial in promoting a more isoelastic implant-bone tissue interface, thereby diminishing the stress shielding effect.

XRD results show that the layers are composed of titanium oxide (anatase and rutile) and the alpha form of tricalcium phosphate phase. As we expected, the intensity of anatase diffraction lines decreased with treatment time. Recent studies show that the best surface for cell culture must be moderately rough and rich in anatase. These can be observed for the sample obtained by MAO at 350V and 3 minutes.

The stability of the oxide film is supported by electrochemical investigation (Tafel plots, EIS and cyclic polarization). The coating obtained after a 3 min oxidation presents the best corrosion behavior because it has a high R_p and a low V_{cor} . The obtained TiO_2 coatings do not present any reactivity until 1,6 V. If we consider that the potential in biological fluids can reach maximum 1V, one can say that this behavior is favorable for medical use.

The results prove a good electrochemical stability, combined with positive behavior regarding its biocompatibility.

Acknowledgements

The authors thank to Cristian Pirvu for kindness and advice about corrosion tests.

This research was supported by CNCSIS grant PD, NO 08/28.07.2010 funded by the Ministry of Education, Research, Youth and Sport, Romania.

R E F E R E N C E S

- [1] *M.S. Kim, J.J. Ryu, Y.M. Sung*, *Electrochem. Commun.*, **vol. 9**, 2007, pp. 1886.
- [2] *Y. Li, I.S. Lee, F.Z. Cui, S.H. Choi*, *Biomaterials*, **vol. 29**, 2008, pp. 2025.
- [3] *D.Y. Kim, M. Kim, H.E. Kim, Y.H. Koh, H.W. Kim, J.H. Jang*, *Acta Biomater.*, **vol. 5**, 2009, pp. 2196.
- [4] *W.H. Song, H.S. Ryu, S.H. Hong*, *J. Biomed. Mater. Res. A*, **vol. 88**, 2009, pp. 246.
- [5] *H. Ishizawa, M. Ogino*, *J. Biomed. Mater. Res.*, **vol. 29**, 1995, pp. 65.
- [6] *X.L. Zhu, K.H. Kim, Y.S. Jeong*, *Biomaterials*, **vol. 22**, 2001, pp. 2199.
- [7] *Y. Han, S.H. Hong, K. Xu*, *Surf. Coat. Technol.*, **vol. 168**, 2003, pp. 249.
- [8] *W.H. Song, Y.K. Jun, Y. Han, S.H. Hong*, *Biomaterials*, **vol. 25**, 2004, pp. 3341.
- [9] *H.T. Chen, C.H. Hsiao, H.Y. Long, C.J. Chung, C.H. Tang, K.C. Chen, J.L. He*, *Surf. Coat. Technol.*, **vol. 204**, 2009, pp. 1126.
- [10] *I. Han, J.H. Choi, B.H. Zhao, H.K. Baik, I.S. Lee*, *Curr. Appl. Phys.*, **vol. 7S1**, 2007, pp. 23.
- [11] *C. Ohtsuki, H. Iida, S. Hayakawa, A. Osaka*, *J. Biomed. Mater. Res.*, **vol. 35**, 2004, pp. 39.
- [12] *Y.T. Sul, C.B. Johansson, Y. Jeong, T. Albrektsson*, *Med. Eng. Phys.*, **vol. 23**, 2001, pp. 329.
- [13] *Y.T. Sul, C.B. Johansson, S. Petronis, A. Krozer, Y. Jeong, A. Wennerberg, T. Albrektsson*, *Biomaterials*, **vol. 23**, 2002, pp. 491.
- [14] *B.C. Yang, J. Weng, X.D. Li, X.D. Zhang*, *J. Biomed. Mater. Res.*, **vol. 47**, 1999, pp. 213.
- [15] *M.B. Pabbruwe, O.C. Standard, C.C. Sorrell, C.R. Howlett*, *Biomaterials*, **vol. 25**, 2004, pp. 4901.
- [16] *L.H. Li, Y.M. Kong, H.W. Kim, Y.W. Kim, H.E. Kim, S.J. Heo, J.Y. Koak*, *Biomaterials*, **vol. 25**, 2004, pp. 2867.
- [17] *X.L. Zhu, J. Chen, L. Scheideler, R. Reichl, J. Geis-Gerstorfer*, *Biomaterials*, **vol. 25**, 2004, pp. 4087.
- [18] *X.B. Chen, Y.C. Li, P.D. Hodgson, C. Wen*, *Mater. Sci. Eng. C*, **vol. 29**, 2009, pp. 165.
- [19] *C. Capuccini, P. Torricelli, F. Sima, E. Boanini, C. Ristoscu, B. Bracci, G. Socol, M. Fini, I.N. Mihailescu, A. Bigi*, *Acta Biomater.*, **vol. 4**, 2008, pp. 1885.
- [20] *Y-T. Sul, C.B. Johansson, S. Petronis, A. Krozer, Y. Jeong, A. Wennerberg, et al.*, *Biomaterials*, **vol. 23**, 2002, pp. 491–501.
- [21] *Y-T. Sul*, *Biomaterials*, **vol. 24**, 2003, pp. 3893–907.
- [22] *Y-T. Sul, C. Johansson, E. Byon, T. Albrektsson*, *Biomaterials*, **vol. 26**, 2005, pp. 6720–30.
- [23] *E. Matykina, M. Montuori, J. Gough, F. Monfort, A. Berkani, P. Skeldon*, *Trans. Inst. Met. Finish*, **vol. 84**, 2006, pp. 125–133.
- [24] *H. Habazaki, K. Shimizu, S. Nagata, P. Skeldon, G.E. Thompson, G.C. Wood*, *Corros. Sci.*, **vol. 44**, 2002, pp. 1047–55.
- [25] *H. Habazaki, K. Shimizu, S. Nagata, P. Skeldon, G.E. Thompson, G.C. Wood*, *J. Electrochem. Soc.*, **vol. 149 B**, 2002, pp. 70–74.
- [26] *H. Habazaki, M. Uozumi, H. Konno, K. Shimizu, P. Skeldon, G.E. Thompson*, *Corros. Sci.*, **vol. 45**, 2003, pp. 2063–2073.

- [27] *E. Matykina, F. Monfort, A. Berkani, P. Skeldon, G.E. Thompson, P. Chapon, Phil. Mag., vol. 86*, 2006, pp. 49–66.
- [28] *E. Matykina, F. Monfort, A. Berkani, P. Skeldon, G.E. Thompson, J. Gough, J. Electrochem. Soc., vol. 154 C*, 2007, pp. 279–285.
- [29] *B. Yoo, K.R. Shin, D.Y. Hwang, D.H. Lee, D.H. Shin, Appl. Surf. Sci., vol. 256*, 2010, pp. 6667.
- [30] *F. Liu, J.L. Xu, D.Z. Yu, F.P. Wang, L.C. Zhao, Mater. Chem. Phys., vol. 121*, 2010, pp. 172.